

Relative Free Energy of Binding and Binding Mode Calculations of HIV-1 RT Inhibitors Based on Dock-MM-PB/GS

Zhigang Zhou, Jeffrey D. Madura*

Department of Chemistry and Biochemistry, Duquesne University, Pittsburgh, PA 15282.

* To whom correspondence should be addressed

e-mail: madura@duq.edu

Phone: 412-396-6341

Fax: 412-396-5683

Keywords:

Binding affinity, docking, Poisson-Boltzmann, solvation energy, solvent-accessible surface, rational drug design, linear response.

Abstract

TIBO derivatives are important non-nucleoside HIV-1 RT inhibitors (NNRTI). Several TIBO derivatives have shown high potency to inhibit RT and one (Tivirapine) has entered into clinical trials. The Free Energy of Binding (FEB) is a numerical way to express the binding affinity of a ligand to its receptor and has been applied in screening candidates in rational drug design. In this work, the FEB of 42 TIBOs in RT was studied. Relative FEB is expressed in the form of a linear combination of vdW, electrostatic, solvation, and nonpolar solvation energy terms. The predicted FEB activity of the TIBOs studied has a good correlation ($r^2=0.8680$, $q^2 = 0.8298$) with respect to the experimental activity (pIC_{50}). Based upon the data reported here, the PB/GS solvation energy term is very important in predicting the binding affinity of TIBOs in RT. In summary, the Dock-MM-PB/GS method is a promising technique in predicting ligand/receptor binding affinity and that it can be used to screen relatively large sets of molecules in a reasonable amount of computer time.

Introduction

The Acquired Immune Deficiency Syndrome (AIDS) claimed over 3 million lives in 2002 with an estimated 5 million people being infected with the Human Immunodeficiency Virus (HIV) each year. To date, no successful cure for the disease has been reported. The Reverse Transcriptase of the Human Immunodeficiency Virus type 1 (HIV-1 RT) is a unique enzyme of the virus that transcribes a single-stranded viral RNA genome into double-stranded DNA, which is subsequently integrated into the host cell genome by an integrase enzyme.¹⁻⁴ RT plays a vital role in the replication of HIV-1 and has been an important target for drug development in treating AIDS. RT is a dimer protein consisting of two related chains: 66kDa (p66) and 51kDa (p51).⁵⁻¹⁰ The p66 subunit resembles a human right hand and thus the four subdomains of p66 are referred to as the thumb, palm, fingers, and connection. The polymerase domain and the RNase H domains are located on the p66 subunit. New DNA is synthesized between the cleft of the thumb and fingers subdomain while a viral RNA strand is held in place as a template.¹¹

Several drugs that target this enzyme have been approved by the FDA for the treatment of AIDS.¹² Two classes of inhibitors have been identified for RT.¹³ The first is a nucleoside analog, in which a nucleoside analog is incorporated into the DNA synthesis by RNase H resulting in chain termination. The nucleoside analog lacks a hydroxyl group and can not react with the nucleoside any more preventing DNA elongation. The second class of inhibitors is the so-called non-nucleoside inhibitor (NNRTI), which bind at an allosteric site on the p66 subdomain, called the non-nucleoside binding pocket (NNBP) (**Figure 1**).^{5,14-20} TIBO and its derivatives are one class of NNRTIs that have demonstrated significant activity for RT inhibition. One TIBO, Tivirapine has entered clinical trials.¹⁶

Several crystal structures of TIBO/RT complexes have been solved.^{8,9,11,21-23} These structures are providing valuable insight into the binding orientations and interactions of TIBOs in RT, but the binding complexes of many other TIBOs are not yet known. Although it is assumed that these structurally similar TIBOs bind in a similar orientation to RT, further exploration of the binding structure of other TIBOs is necessary to understand the mechanism of inhibition and to aid in the design of more potent inhibitors that are effective to RT mutants which emerge when HIV is exposed to a NNRTI.

An alternative way to predict the binding structure of a substrate in its receptor is by a docking simulation, which has been successfully used in many applications.²⁴⁻³² Some docking methods have demonstrated promising power to predict reasonable binding structures. Combinations of the docking method with other techniques, such as MD simulation, free energy calculation, comparative molecular field analysis (CoMFA),³³ and comparative molecular similarity indices analysis (CoMSIA)^{34,35} can provide valuable insights into biological systems and aid in rational drug design.³⁶⁻⁴⁵ Several ways in calculating the free energy of binding (FEB) have been suggested and used in different applications. In one approach, Jorgensen, et al. have successfully applied Monte Carlo and Linear Response Equation (LRE) to calculate the binding affinities of many systems.⁴⁶⁻⁵² The free energy perturbation (FEP) and thermodynamic integration (TI) approaches have been used to estimate accurate free energy values. However, to obtain accurate results from a sufficient statistical sampling, these methods require lots of computer time and therefore they⁵³ are normally suitable for small sample sets.

Wang, et al. developed MM-PBSA and applied the method to predict the activity of 12 TIBO-like inhibitors.⁵⁴⁻⁵⁷ A reasonable correlation between the calculated FEB and experimental activity was obtained from their calculations. The MM-PBSA method obtains a statistic average

energy over a number of structures sampled from MD snapshots. It is a useful tool to analyze energetic properties in the post-processing of a MD simulation. However, the procedure requires an MD simulation to sample a number of binding structures followed by a calculation of the energies for all of the structures. For a sample set containing a large number of ligands, this method is still very time-consuming.

Recently, other alternative methods have been developed to estimate the binding free energies, including CMC-MD, the linear interaction method, and “Ludi”-like approaches. These have successfully been used to produce reasonable FEB in selected cases.⁵⁸ Many works have shown that Poisson-Boltzmann and generalized-Born models are good ways to estimate the electrostatic part of the solvation effect in a binding process. Although some work demonstrates that the normal mode analysis can be used to estimate the entropy effect in a process, it is also very time-consuming.^{54,55,59} The entropy contribution is relatively small for less flexible molecules and can be cancelled out in relative free energy calculations. The entropy contribution is usually ignored in most cases. To further develop and apply the approach, we have applied our method to large set of molecules.

In this work, 42 TIBO-like NNRTIs/RT systems were used to test our approach and further develop a fast and convenient way to calculate the FEB of a large set of ligands in their receptor. We first used a flexible docking method (Autodock3)⁶¹ to predict the “preferable” binding structure of the ligands in RT. Then we used traditional MM methods to calculate ligand-receptor interaction energies (ΔE_{ele} , ΔE_{vdW}), the Finite Difference Poisson Boltzmann with a Gaussian Smooth Dielectric Constant Function method (PB/GS) for the electrostatic component of the solvation energy, and the solvent-accessible surface for the nonpolar part of the solvation energy (ZAP program).^{62,63} As stated earlier, the entropy is relatively small for a set of relatively

rigid molecules and can be ignored in this case. Therefore the calculation of entropy is not included in our method. Because the binding energies are obtained using empirical force fields, it is reasonable to scale these energies when using them to estimate free energy. So a linear combination (or linear response) strategy was used to express FEB using different energy components. A number of different scoring functions have been developed using a similar strategy, in which a training set of molecules were used to obtain the necessary scaling factors.⁷³ Our approach is simple, fast and straightforward. It is most advantageous for evaluating the activities of large sets of molecules, where calculation of relative binding affinities is needed.

Methods

Data Set and Coordinates Preparation. The starting coordinates of the HIV-1 RT/TIBO complex (1REV)²² were taken from the Protein Data Bank (www.rcsb.org). After hydrogen atoms were added, the substrate (9CI-TIBO) and the protein (RT) were saved separately using Molecular Operating Environment (MOE) program (Chemical Computing Group, Montreal, Canada). Amber94 force field⁶⁴ was used to assign the partial charges on the protein and for all structure minimizations. A structure minimization was performed to relax these newly added hydrogen atoms by fixing all other non-hydrogen atoms. The minimized structure of the protein was used in later docking simulations. All other substrates were built using the 9CI-TIBO as a template. PEOE charge⁶⁵ was used for these substrates and full optimization was performed to minimize each structure. The minimized structure was used in docking simulations. The structure and activity of the 42 compounds used in this work are listed in **Table I.**⁶⁶⁻⁷⁰

Docking Simulation. Autodock3⁶¹ was used to perform the docking simulation. All single bonds of the substrates were treated as flexible and allowed to rotate freely. The Lamarckian Genetic Algorithm (LGA) in Autodock3 was chosen to perform the docking simulation.⁷¹ The hybrid search technique consists of a global optimizer modified from a genetic algorithm with a 2-point crossover and random mutation and a local optimizer with a Solis and Wets algorithm.⁷² Random seed was used for initial quaternion, coordinates, and torsions. A 0.2 Å step was used for translation and a 25-degree step was used for quaternion and torsion. The maximum number of energy evaluation was 250,000 and the maximum number of generations was 27,000. The rate of gene mutation was 0.02 and the rate of crossover was 0.8. A docking box of 60x60x60 points with a grid spacing of 0.375 Å was used in the calculations. The run number of individuals in the population was set to 20, thus a total of 20 docking configurations were determined for each

docking calculation. The choice of a “preferable” docking configuration was based on the values of the binding free energy and the number of configurations in a cluster.⁶⁰

Poisson-Boltzmann Solvation and Solvent-accessible Surface Calculations. Continuum solvation method numerically solved by Finite Difference Poisson-Boltzmann (PB) with a Gaussian Smooth Dielectric Constant Function method (PB/GS)^{62,63} was used to estimate the solvation energy effect on the binding process of an NNRTI into RT. In the continuum solvation model, different dielectric constants were used in the solvent areas and solute areas. For a collection of point charges, the electrostatic effect acting on a given charge by all other charges can be expressed by Poisson’s equation as follows:

$$\nabla \cdot \mathbf{e}(\mathbf{r}) \nabla \cdot \mathbf{f}(\mathbf{r}) + \mathbf{r}(\mathbf{r}) = 0 \quad (1)$$

where \mathbf{r} is the position vector, \mathbf{r} is the charge density, \mathbf{f} is the electrostatic potential and \mathbf{e} is the dielectric constant. The latter three are the functions of the position vector \mathbf{r} . Different methods use different functions to determine the dielectric constant and the charge values at the boundary between solute and solvent. For example, UHBD uses a distance-dependent interpolation to calculate the dielectric constant and the charge values at the boundary. PB/GS uses a Gaussian representation to describe the variation of the dielectric constant for a solute in a continuum solvent. A smooth variation of dielectric constant from low values inside the solute to high values in bulk solvent is obtained by Gaussian. The Gaussian of charge density (\mathbf{r}_A) is given by the following equation:

$$\mathbf{r}_A(\mathbf{r}) = p_A \exp(-kr_A^2/\sigma_A^2) \quad (2)$$

where p_A is a height factor, r_A is the radial distance from atom A , and k is a dimensionless exponent. The charge density for a molecule can be expressed by:

$$\mathbf{r}_{\text{mol}}(\mathbf{r}) = 1 - \prod_A (1 - \mathbf{r}_A(\mathbf{r})) \quad (3)$$

This equation can be expanded into:

$$\begin{aligned}\mathbf{r}_{\text{mol}}(\mathbf{r}) &= \sum_A \mathbf{r}_A(\mathbf{r}) - \sum_{A>B} \mathbf{r}_A(\mathbf{r})\mathbf{r}_B(\mathbf{r}) + \dots \\ &= \mathbf{r}_{\text{sum}}(\mathbf{r}) + \text{“intersection terms”}\end{aligned}\quad (4)$$

where $\mathbf{r}_{\text{sum}}(\mathbf{r})$ is the linear summation of all atomic terms.

Therefore the spatial variation in the dielectric constant can be expressed by the following function:

$$\mathbf{e}(\mathbf{r}) = \mathbf{e}_{\text{solute}} + (\mathbf{e}_{\text{solvent}} - \mathbf{e}_{\text{solute}}) \exp(-A\mathbf{r}_{\text{sum}}(\mathbf{r})) \quad (5)$$

where A is a suitable constant, and both $\mathbf{e}_{\text{solute}}$ and $\mathbf{e}_{\text{solvent}}$ are dielectric constants of solute and solvent, respectively. The total charge contained within the grid cell ijk is expressed in the following grid integral:

$$Q_{ijk} = \int_{V_{ijk}} d\mathbf{r} \mathbf{r}_{\text{mol}}(\mathbf{r}) \quad (6)$$

A linearized PB equation can be written in the following form:

$$\nabla \cdot \mathbf{e}(\mathbf{r}) \nabla \cdot \mathbf{f}(\mathbf{r}) = -\mathbf{r}(\mathbf{r}) - k_0^2 \mathbf{f}(\mathbf{r}) \quad (7)$$

where k_0 is a constant as follows:

$$k_0^2 = 2e^2 N_A \mathbf{r}_0 / kT \quad (8)$$

The linearized PB equation 7 is solved by the Finite Difference method based on a grid map.

To save computer time with an effort to sacrifice as little accuracy as possible, a focusing technique was used to solve the PB equation for macromolecules. A coarse grid is applied on the whole protein and a finer grid is applied around the binding site. The boundary condition of the finer grid is obtained from a calculation result from the coarse grid. In this work, a grid spacing

of 0.25 Å and 3 Å were used for the finer and the coarse grid, respectively. Dielectric constants of 2 and 80 were used for protein and water, respectively.

The nonpolar solvation contribution (ΔG_n) in a binding process of a ligand in its receptor is estimated by the solvent-accessible surface area buried by the complex, which is calculated by the grid-based Gaussian smoothing technique as given below:

$$\Delta G_n = g \Delta A \quad (9)$$

where g is the energy coefficient of every unit surface area change when non-polar solutes transfer from a low-dielectric solvent to the high dielectric solvent, such as water. The empirical value of g is normally determined by a trial set of molecules. Different values have been suggested for different applications.

MM and Binding Free Energies. The structure minimization and MM energy calculation were performed using the MOE program. AMBER94 force field⁶⁴ was used. A combination of minimization protocols, which consists of Steepest Descent (SD), Conjugate Gradient (CG), and Truncated Newton (TN) methods, were used in all minimizations. In the protocol, the RMSD gradient limits in SD, CG, and TN were 1000, 100, and 0.1, respectively. The iteration limits in SD, CG, and TN were 100, 100, and 300, respectively.

After a preferable binding structure was obtained from docking simulation, the complex was partially minimized by relaxing the ligand and the side chains that were within 7Å from the ligand while all other atoms were fixed. After all energies were calculated, factor analysis (FA) and multiple regression analysis (MRA) were used to derive a LRE-like equation:

$$\Delta G^b (\text{FEB}) = w_1 \Delta G_{\text{vdW}}^b + w_2 \Delta G_{\text{ele}}^b + w_3 \Delta G_{\text{solv}}^b + w_4 \Delta G_n^b \quad (10)$$

where w_1 , w_2 , w_3 , and w_4 are weight factors. ΔG^b is binding energy, which is energy difference between ligand/receptor complex and free protein and ligand:

$$\Delta G^b = \Delta G_{\text{complex}} + \Delta G_{\text{protein}} + \Delta G_{\text{ligand}} \quad (11)$$

Results and Discussions

9CI-TIBO docking back its binding site. As stated earlier, the coordinates of RT from 1REV were used in this work. To validate the docking protocol, 9CI-TIBO from the complex (1REV) was docked into its original structure of RT. After the ligand was removed from the binding site and placed at the binding site entrance, a docking simulation was performed. The docking result is listed in **Table II**. Out of the 20 configurations from the docking simulation, 19 configurations (No.1- No.19) were very similar in binding orientation as compared to the crystal complex with a root mean square deviation (RMSD) of smaller than 1.2Å. Only one configuration had a large RMSD of 2.148 Å compared to the crystal structure. The $\Delta G_{\text{binding}}$ estimated from the docking simulation shows that 18 out of 20 configurations have nearly the same FEB value with a maximum difference of 0.18 kcal/mol (relative difference, 1.6%). Also the docked energy of 18 configurations is nearly the same with the maximum difference of 0.35 kcal/mol (relative difference, 2.6%). All of these docked configurations were superimposed onto the original crystal structure (**Figure 2**). It can be seen that, 18 of the 20 configurations bind in the same orientation with a very similar position as compared to the RT crystal structure. There is only one which binds in a different orientation from the crystal structure. It is demonstrated that the docking simulation reproduces the binding structure and orientation of the ligand in its crystal structure very well. In our previous work, similar docking simulations produced similar satisfactory results.^{27,60} Therefore, this docking simulation protocol is used to dock all other TIBOs into RT to find their binding structures and interaction energies.

Docking of the molecule set. After the validation of the docking method using 9CI-TIBO, all other molecules were docked into the same coordinates of RT. The same docking protocol was used for all docking calculations. In each docking simulation, 20 configurations were

obtained and were grouped into different clusters, where a cluster is defined as a group of positions that has a RMSD of $< 1 \text{ \AA}$ for non-hydrogen atoms. Shown in **Table III** are the docking results of all sets of molecules in which data related to the cluster and FEB are reported. From these results, it can be seen that there are 1-3 clusters in each simulation. In most cases more than half of the configurations fall into the major cluster such that the ligand binds inside of the NNRTI binding pocket of RT. Of the 42 docking simulations, 28 (67%) have more than 15 configurations in their major cluster; 40 (95%) have more than 10 (50%) configurations in their major cluster. The result demonstrates that the docking simulation can dock these TIBO inhibitors back into the NNRTI binding site well. By visually checking the docking positions and orientations, it is seen that in a major cluster, all configurations from the docking bind in the same orientation and with very similar positions. The few number of clusters in each docking simulation could mean that the simulation does not sufficiently sample configuration space. By superimposing the “preferable” binding configuration of all molecules from their major clusters, we can see that these molecules bind in the same orientation and in a similar position with respect to the tricyclic ring system. Since these molecules all have the same tricyclic ring moiety, it is expected that they will bind in a similar pattern in the NNRTI binding site of RT. Several available crystal RT/TIBO complexes show that they have low RMSD for common structures after the complexes are superimposed together. Based on all of this evidence we are confident that the docking results can be used for further calculations.

FEB was estimated from the Autodock3 results. All of the docked complexes in the major cluster had very similar FEB values. The average FEB (the value before \pm) and the range (the value after \pm) are listed in **Table III**. For most complexes, the relative change was within 3%.

Although we obtained reasonable FEB values from the Autodock3 simulations, represented by a reasonable linear correlation ($r^2=0.724, 0.973$, respectively) with respect to the experimental activities as demonstrated in our two previous docking calculations,^{27,60} the FEB seems to have no reasonable correlation to their activity (pIC_{50}) in this work. The pIC_{50} for the set of TIBOs studied varies over a large range, from 3.24 to 8.52. But the calculated FEB varies in a narrow range from -10.0 to -12.6 kcal/mol.

Calculated Free Energy vs. Activity. In each docking simulation, the “preferable” structure was picked as the docked structure to be used in the FEB calculations. Since Autodock3 treats a receptor rigidly during the docking simulation, an energy minimization, neglecting a solvation term, was performed on the preferred docked complex. The vdW and electrostatic energy between the ligand and the receptor was calculated for each minimized complex. Also a desolvation energy and solvent accessible surface area (SASA) change was calculated using ZAP.^{62,63} These energies are listed in **Table IV**. A graph of these energies vs. activity (pIC_{50}) of the ligands showed inconsistent correlation to the experimental activity for all ligands. A scheme similar to Linear Response was used to develop a FEB relationship based on these energies, which can express the activity of these TIBOs. Multiple regression analysis was performed using Statistica (StatSoft, Inc). The properties of the final regression model are listed in **Table V**. From the results of the correlation factor analysis, it can be seen that SASA has the most significant correlation to the experimental activity (pIC_{50}) with a correlation coefficient of 0.86, and the electrostatic energy (G_{ele}) has a less significant correlation to the activity with a correlation coefficient of 0.08. It indicates that in the binding of these TIBOs, non-polar solvation may be a major driving force in their binding and may contribute to increased activity. The correlation between predicted activity and actual activity is shown in **Figure3**. The calculated activity has

good correlation to the actual activity with a correlation coefficient (r) of 0.93 ($r^2=0.87$). The FEB expression accounts for nearly 87% of the variance of these four energy components. The predictiveness of the model was further assessed using cross-validation method (leave-one-out). The result shows that the model has good predictability to the activity with a cross-validation coefficient (q) of 0.9109 ($q^2 = 0.8298$).

As stated early, the major interest in drug design is to express the variance of free energy over a set of active molecules. The scaled energies produce a reasonable value for the FEB, by which an activity (pIC_{50}) was calculated. The residues between the calculated and experimental activities for all compounds are depicted in **Figure 4**. The calculated activities were satisfactory with deviations of < 1 compared to the experimental activity (pIC_{50}).

Biological Implications of the Docked Structure. The docked complexes of all compounds show that they bind in a very similar pattern in RT. To illustrate the binding structures of compounds with different activity, we superimposed the four ligands showing the highest activities as follows: TIBO2 (dark green, $pIC_{50}=7.47$), TIBO3 (red, $pIC_{50}=8.37$) TIBO10 (light green, $pIC_{50}=8.52$), and TIBO21 (purple, $pIC_{50}=7.60$). Two ligands showing the lowest activities were also evaluated in the NNRTI binding site: TIBO26 (colored by element, $pIC_{50}=3.24$) and TIBO33 (colored by element, $pIC_{50}=4.00$) (**Figure 5**). For clarity, not all of the ligands are included in the figure. It can be seen that at the 8 or 9 position, the X-substituent of these sample ligands is located in a fairly similar position. The location of the Z-substituent of these sample ligands seems to have no relation to their activity. There is no apparent binding difference between the highly active ligands and less active ligands. So, the binding position and orientation can not be used to explain the activity difference. In the energy calculation, we also explained that the vdW energy does not significantly contribute the activity difference. Thus,

other effects, such as solvation have a significant contribution to the activity difference of this family NNRTIs. This suggests that the hydrophobic property of a NNRTI is important to its activity. This property is the driving force for the binding of a NNRTI into the allosteric pocket of RT.

Conclusions

We have presented herein a FEB method for the binding affinity of 42 TIBO-like non-nucleoside HIV-1 RT inhibitors. The binding structures of these ligands in RT were predicted by flexible docking simulations. These docking calculations demonstrate that docking simulations can satisfactorily reproduce a bound complex from a crystal structure of the RT/TIBO complex. Superposition of the calculated binding complexes for the entire set of ligands from docking simulations, shows that structurally similar ligands bind in a very similar pattern. The ligands bind in the same orientation as found in crystal structures of RT/TIBO. All of the ligands bind in a similar position inside the NNRT binding site of RT and are found to fit the binding pocket well.

The calculated FEB for these ligands reasonably predicted the activity for this family of ligands. The calculated activity has good correlation to the experimental activity with a correlation coefficient (r) of 0.9317 and cross-validation coefficient (q) of 0.9109. Using an optimized linear combination of four energy terms, vdW, electrostatic, solvation (electrostatic part), and nonpolar energies, the binding affinity for a large set of ligands in the receptor can be accurately and rapidly determined. The Dock-MM-PB/GS combination demonstrates that a reasonable binding structure can be identified and that the calculated binding energy is reasonably determined. The PB/GS method predicted reasonable solvation energy terms, which enabled a satisfactory FEB expression to be built. In this work, it was noticed that among these energy terms, the ligand solvation (electrostatic and nonpolar) plays a major role on the determination of the activity of TIBOs.

This work suggests that in a relative FEB calculation, which is of major interest in drug design, the contribution of different energy terms can be scaled by a set of weighting factors to

determine the correlation. In practice, it is known that the same energy term plays different roles in different type of systems. This is one of the reasons that reasonable activity models can be obtained based on different energy terms. The work reported here successfully applies a modified MM/PBSA method^{54-57,60}, which can be applied to a large set of molecules.

The calculation of the change in solvation upon ligand binding in a protein is a challenging problem. This study as well as many others has shown that the solvation effect is an important driving force on ligand binding and a key factor in the expression of activity of a set of ligands. An accurate and fast method to directly calculate solvation energy (all effects) still remains an important challenge.

Acknowledgements

The authors would like to thank Dr. Athony Nicholls for his generosity to provide ZAP program and Dr Mikell Paige for his assistant on manuscript preparation. This research was supported in part by a grant from the National Computational Science Alliance (MCB990008Nr00).

References:

1. Jacobo-Molina A, Arnold E. HIV reverse transcriptase structure-function relationships. *Biochemistry* 1991;30:6351-6361.
2. Le Grice SFJ. Human immunodeficiency virus reverse transcriptase. In: Skalka AM GS, editor. *Reverse transcriptase*. Plainview, NY: Cold spring Harbor Laboratory Press; 1993. p 163-191.
3. Goff P. Retroviral reverse transcriptase: Synthesis, structure and function. *J Acquired Immune Deficiency Syndromes* 1990;3:817-831.
4. Whitcomb JM, Hughes SH. Retroviral reverse transcription and integration: Progress and problems. *Annu Rev Cell Biol* 1992;8:275-306.
5. Tantillo C, Ding J, Jacobo-Molina A, Nanni RG, Boyer PL, Hughes SH, Pauwels R, Andries K, Janssen PAJ, Arnold E. Locations of anti-AIDS drug binding sites and resistance mutations in the three-dimensional structure of HIV-1 reverse transcriptase: implications for mechanisms of drug inhibition and resistance. *J Mol Biol* 1994;243:369-387.
6. Kohlstaedt LA, Wang J, Friedman JM, Rice PA, Steitz TA. Crystal structure at 3.5Å resolution of HIV-1 reverse transcriptase complexed with an inhibitor. *Science* 1992;256:1783-1790.
7. Smerdon SJ, Jager J, Wang J, Kohlstaedt LA, Chirino AJ, Friedman JM, Rice PA, Steitz TA. Structure of the binding site for nonnucleoside inhibitors of reverse transcriptase of human immunodeficiency virus type 1. *Proc Natl Acad Sci* 1994;91:3911-3915.
8. Ding J, Das K, Moereels H, Koymans L, Andries K, Janssen PA, Hughes SH, Arnold E. Structure of HIV-1 RT/TIBO R 86183 reveals similarity in the binding of diverse nonnucleoside inhibitors. *Nature Struct Biol* 1995;2:407-415.
9. Ding J, Das K, Tantillo C, Zhang W, Jr. ADC, Jessen S, Lu X, Hsiou Y, Jacobo-Molona A, Andries K, Pauwels R, Moereels H, Koymans L, Janssen PA, Smith R, Koepke MK, Michejda C, Hughes SH, Arnold E. Structure of HIV-1 reverse transcriptase in a complex with the nonnucleoside inhibitor a-APA R 95845 at 2.8Å resolution. *Structure* 1995;3:365-379.
10. Jacobo-Molina A, Ding J, Nanni RG, Jr. ADC, Lu X, Tamtilo C, Williams RL, Kamer G, Ferris AL, Clark P, Hizi A, Hughes SH, Arnold E. Crystal structure of human immunodeficiency virus type 1 reverse transcriptase complexed with double-stranded DNA at 3.0Å resolution shows bent DNA. *Proc Natl Acad Sci* 1993;90:6320-6324.
11. Huang H, Chopra R, Verdine GL, Harrison SC. Structure of a Covalently Trapped Catalytic Complex of HIV-1 Reverse Transcriptase: Implications for Drug Resistance. *Science* 1998;282(27):1669-1675.
12. <http://www.niaid.nih.gov/daids/dtpdb/fdadrug.htm>.
13. Garg R, Gupta SP, Gao H, Babu MS, Debnath AK, Hansch C. Comparative Quantitative Structure-Activity Relationship Studies on Anti-HIV Drugs. *Chem Rev* 1999;99(12):3525-3602.
14. Arnold E, Das K, Ding J, Yadav P, Hsiou Y, Boyer PL, Hughes SH. Targeting HIV reverse transcriptase for anti-AIDS drug design: structural and biological considerations for chemotherapeutic strategies. *Drug Design Discov* 1996;13:29-47.
15. Larder BA. Inhibitors of HIV reverse transcriptase as antiviral agents and drug resistance. In: Skalka AM GS, editor. *Reverse Transcriptase*. Plainview, NY: Cold spring Harbor Laboratory Press; 1993. p 163-191.
16. De Clercq E. Antiviral therapy for human immunodeficiency virus infections. *Clin Microbiol Rev* 1995;8:200-239.
17. Ding J, Das K, Hsiou Y, Zhang W, Arnold E, Yadav PNS, S.H.Hughes. Structural Studies of HIV-1 Reverse Transcriptase and Implications for Drug Design. *Structure-Based Drug Design* 1997: 41-82.
18. Pedersen OS, Pedersen EB. non-nucleoside reverse transcriptase inhibitors. *Antiviral Chem Chemother* 1999;10:285-314.
19. Koup RA, Merluzzi VJ, Hargrave kD, Adems J, Grozinger K, Eckner RJ, Saivan JL. Inhibition of human immunodeficiency virus type1 replication by the dipyridociazepinone BI-RG-587. *J infect Dis* 1991;163:966-970.
20. Richman D, Rosenthal AS, Shoog M, Eckner RJ, Chou TC, Sabo JP, Merluzzi VJ. BI-RG-587 in active against zidovudine-pesistant human immunodeficiency virus type 1 and synergistic with zidovudine. *Antimicrob Agents chemother* 1991;35:305-308.
21. Das K, Ding J, Hsiou Y, Clark AJ, Moereels H, Koymans L, Andries K, Pauwels R, Janssen P, Boyer P, Clark P, Smith RJ, Kroeger SM, Michejda C, Hughes S, Arnold E. Crystal structures of 8-Cl and 9-Cl

- TIBO complexed with wild-type HIV-1 RT and 8-Cl TIBO complexed with the Tyr181Cys HIV-1 RT drug-resistant mutant. *J Mol Biol* 1996;264(4):1085-1100.
22. Ren J, Esnouf R, Hopkins A, Ross C, Jones Y, Stammers D, Stuart D. The structure of HIV-1 reverse transcriptase complexed with 9-chloro-TIBO: lessons for inhibitor design. *Structure* 1995;3(9):915-926.
 23. Hsiou Y, Ding J, Das K, Jr. ADC, Hughes SH, Arnold E. Structure of unliganded HIV-1 reverse transcriptase at 2.7 Å resolution: implications of conformational changes for polymerization and inhibition mechanisms. *Structure* 1996;4:853-860.
 24. Dominguez C, Boelens R, Bonvin AMJJ. HADDOCK: A Protein-Protein Docking Approach Based on Biochemical or Biophysical Information. *Journal of the American Chemical Society* 2003;125(7):1731-1737.
 25. Jain AN. Surflex: Fully Automatic Flexible Molecular Docking Using a Molecular Similarity-Based Search Engine. *Journal of Medicinal Chemistry* 2003;46(4):499-511.
 26. Johnson MA, Hoeog C, Pinto BM. A Novel Modeling Protocol for Protein Receptors Guided by Bound-Ligand Conformation. *Biochemistry* 2003;42(7):1842-1853.
 27. Zhou Z, Fisher D, Spidel J, Greenfield J, Patson B, Fazal A, Wigal C, Moe OA, Madura JD. Kinetic and Docking Studies of the Interaction of Quinones with the Quinone Reductase Active Site. *Biochemistry* 2003;42(7):1985-1994.
 28. Wu X, Milne JLS, Borgnia MJ, Rostapshov AV, Subramaniam S, Brooks BR. A core-weighted fitting method for docking atomic structures into low-resolution maps: Application to cryo-electron microscopy. *Journal of Structural Biology* 2003;141(1):63-76.
 29. Todorov NP, Mancera RL, Monthoux PH. A new quantum stochastic tunnelling optimisation method for protein-ligand docking. *Chemical Physics Letters* 2003;369(3,4):257-263.
 30. Wang L, Merz AJ, Collins KM, Wickner W. Hierarchy of protein assembly at the vertex ring domain for yeast vacuole docking and fusion. *Journal of Cell Biology* 2003;160(3):365-374.
 31. Vicker N, Ho Y, Robinson J, Woo LLW, Purohit A, Reed MJ, Potter BVL. Docking studies of sulphamate inhibitors of estrone sulphatase in human carbonic anhydrase II. *Bioorganic & Medicinal Chemistry Letters* 2003;13(5):863-865.
 32. Sabnis YA, Desai PV, Rosenthal PJ, Avery MA. Probing the structure of falcipain-3, a cysteine protease from plasmodium falciparum: Comparative protein modeling and docking studies. *Protein Science* 2003;12(3):501-509.
 33. Cramer RDI, Patterson DE, Bunce JD. Comparative molecular field analysis (CoMFA). 1. Effect of shape on binding of steroids to carrier proteins. *J Am Chem Soc* 1988;110(18):5959-5967.
 34. Klebe G, Abraham U, Mietzner T. Molecular Similarity Indices in a Comparative Analysis (CoMSIA) of Drug Molecules to Correlate and Predict Their Biological Activity. *J Med Chem* 1994;37(24):4130-4146.
 35. TBohm M, Sturzebecher J, Klebe G. hree-Dimensional Quantitative Structure-Activity Relationship Analyses Using Comparative Molecular Field Analysis and Comparative Molecular Similarity Indices Analysis To Elucidate Selectivity Differences of Inhibitors Binding to Trypsin, Thrombin, and Factor Xa. *J Med Chem* 1999;42(3):458-477.
 36. Buolamwini JK, Assefa H. CoMFA and CoMSIA 3D QSAR and Docking Studies on Conformationally-Restrained Cinnamoyl HIV-1 Integrase Inhibitors: Exploration of a Binding Mode at the Active Site. *Journal of Medicinal Chemistry* 2002;45(4):841-852.
 37. Nair AC, Jayatilleke P, Wang X, Miertus S, Welsh WJ. Computational studies on tetrahydropyrimidine-2-one HIV-1 protease inhibitors: improving three-dimensional quantitative structure-activity relationship comparative molecular field analysis models by inclusion of calculated inhibitor- and receptor-based properties. *Journal of Medicinal Chemistry* 2002;45(4):973-983.
 38. Pungpo P, Hannongbua S. Three-dimensional quantitative structure-activity relationships study on HIV-1 reverse transcriptase inhibitors in the class of dipyrindiazepinone derivatives, using comparative molecular field analysis. *Journal of Molecular Graphics & Modelling* 2000;18(6):581-590.
 39. Jayatilleke PRN, Nair AC, Zauhar R, Welsh WJ. Computational Studies on HIV-1 Protease Inhibitors: Influence of Calculated Inhibitor-Enzyme Binding Affinities on the Statistical Quality of 3D-QSAR CoMFA Models. *Journal of Medicinal Chemistry* 2000;43(23):4446-4451.
 40. Barreca ML, Carotti A, Carrieri A, Chimirri A, Monforte AM, Calace MP, Rao A. Comparative molecular field analysis (CoMFA) and docking studies of non-nucleoside HIV-1 RT inhibitors (NNIs). *Bioorganic & Medicinal Chemistry* 1999;7(11):2283-2292.
 41. Hilgeroth A, Fleischer R, Wiese M, Heinemann FW. Comparison of azacyclic urea A-98881 as HIV-1 protease inhibitor with cage dimeric N-benzyl 4-(4-methoxyphenyl)-1,4-dihydropyridine as representative

- of a novel class of HIV-1 protease inhibitors: a molecular modeling study. *Journal of Computer-Aided Molecular Design* 1999;13(3):233-242.
42. Debnath AK. Three-Dimensional Quantitative Structure-Activity Relationship Study on Cyclic Urea Derivatives as HIV-1 Protease Inhibitors: Application of Comparative Molecular Field Analysis. *Journal of Medicinal Chemistry* 1999;42(2):249-259.
 43. Raghavan K, Buolamwini JK, Fesen MR, Pommier Y, Kohn KW, Weinstein JN. Three-Dimensional Quantitative Structure-Activity Relationship (QSAR) of HIV Integrase Inhibitors: A Comparative Molecular Field Analysis (CoMFA) Study. *Journal of Medicinal Chemistry* 1995;38(6):890-897.
 44. Oprea TI, Waller CL, Marshall GR. 3D-QSAR of human immunodeficiency virus (I) protease inhibitors. III. Interpretation of CoMFA results. *Drug Design and Discovery* 1994;12(1):29-51.
 45. Debnath AK, Jiang S, Strick N, Lin K, Haberfield P, Neurath AR. Three-Dimensional Structure-Activity Analysis of a Series of Porphyrin Derivatives with Anti-HIV-1 Activity Targeted to the V3 Loop of the gp120 Envelope Glycoprotein of the Human Immunodeficiency Virus Type 1. *Journal of Medicinal Chemistry* 1994;37(8):1099-1108.
 46. Smith MBK, Lamb ML, Tirado-Rives J, Jorgensen WL, Michejda CJ, Ruby SK, Smith RH, Jr. Monte Carlo calculations on HIV-1 reverse transcriptase complexed with the non-nucleoside inhibitor 8-Cl TIBO: contribution of the L100I and Y181C variants to protein stability and biological activity. *Protein Engineering* 2000;13(6):413-421.
 47. Smith RH, Jr., Jorgensen WL, Tirado-Rives J, Lamb ML, Janssen PAJ, Michejda CJ, Smith MBK. Prediction of Binding Affinities for TIBO Inhibitors of HIV-1 Reverse Transcriptase Using Monte Carlo Simulations in a Linear Response Method. *Journal of Medicinal Chemistry* 1998;41(26):5272-5286.
 48. Eriksson MAL, Pitera J, Kollman PA. Prediction of the binding free energies of new TIBO-like HIV-1 reverse transcriptase inhibitors using a combination of PROFEC, PB/SA, CMC?MD, and free energy calculations. *J Med Chem* 1999;42:868-881.
 49. Essex JW, Severance DL, Tirado-Rives J, Jorgensen WL. Monte Carlo Simulations for Proteins: Binding Affinities for Trypsin-Benzamidine Complexes via Free-Energy Perturbations. *Journal of Physical Chemistry B* 1997;101(46):9663-9669.
 50. Jorgensen WL, Duffy EM. Prediction of drug solubility from Monte Carlo simulations. *Bioorganic & Medicinal Chemistry Letters* 2000;10(11):1155-1158.
 51. Jorgensen WL, Price MLP, Price DJ, Rizzo RC, Wang D, Pierce AC, Tirado-Rives J. COX-2, SRC, SH2 domain, HIV reverse transcriptase, and thrombin: Computational approaches to protein-ligand binding. *Free Energy Calculations in Rational Drug Design* 2001:299-316.
 52. Price MLP, Jorgensen WL. Analysis of binding affinities for celecoxib analogues with COX-1 and COX-2 from combined docking and Monte Carlo simulations and insight into the COX-2/COX-1 selectivity. *Journal of the American Chemical Society* 2000;122(39):9455-9466.
 53. Kollman PA. Free energy calculations: Applications to chemical and biochemical phenomena. *Chemical Reviews* (Washington, DC, United States) 1993;93(7):2395-2417.
 54. Wang J, Morin P, Wang W, Kollman PA. Use of MM-PBSA in Reproducing the Binding Free Energies to HIV-1 RT of TIBO Derivatives and Predicting the Binding Mode to HIV-1 RT of Efavirenz by Docking and MM-PBSA. *Journal of the American Chemical Society* 2001;123(22):5221-5230.
 55. Wang W, Lim WA, Jakalian A, Wang J, Wang J, Luo R, Bayly CI, Kollman PA. An analysis of the interactions between the Sem-5 SH3 domain and its ligands using molecular dynamics, free energy calculations, and sequence analysis. *Journal of the American Chemical Society* 2001;123(17):3986-3994.
 56. Kuhn B, Donini O, Huo S, Wang J, Kollman PA. MM-PBSA applied to computer-assisted ligand design. *Free Energy Calculations in Rational Drug Design* 2001:243-251.
 57. Kollman PA, Massova I, Reyes C, Kuhn B, Huo S, Chong L, Lee M, Lee T, Duan Y, Wang W, Donini O, Cieplak P, Srinivasan J, Case DA, Cheatham TE, III. Calculating Structures and Free Energies of Complex Molecules: Combining Molecular Mechanics and Continuum Models. *Accounts of Chemical Research* 2000;33(12):889-897.
 58. Zou X, Sun Y, Kuntz ID. Inclusion of Solvation in Ligand Binding Free Energy Calculations Using the Generalized-Born Model. *Journal of the American Chemical Society* 1999;121(35):8033-8043.
 59. Yan S, Shapiro R, Geacintov NE, Broyde S. Stereochemical, Structural, and Thermodynamic Origins of Stability Differences between Stereoisomeric Benzo[a]pyrene Diol Epoxide Deoxyadenosine Adducts in a DNA Mutational Hot Spot Sequence. *Journal of the American Chemical Society* 2001;123(29):7054-7066.
 60. Zhou Z, Madrid M, Madura JD. New Non-nucleoside Inhibitors in HIV-1 RT Docking Calculations. *Proteins: Structure, Function Genetics* 2002;49(4):529-542.

61. Jones G, Willett P, Glen RC, Leach AR, Taylor R. Development and validation of a genetic algorithm for flexible docking. *Journal of Molecular Biology* 1997;267(3):727-748.
62. Grant JA, Pickup BT, Nicholls A. A smooth permittivity function for poisson-boltzmann solvation methods. *Journal of Computational Chemistry* 2001;22(6):608-640.
63. Rocchia W, Sridharan S, Nicholls A, Alexov E, Chiabrera A, Honig B. Rapid grid-based construction of the molecular surface and the use of induced surface charge to calculate reaction field energies: applications to the molecular systems and geometric objects. *Journal of Computational Chemistry* 2002;23(1):128-137.
64. Weiner SJ, Kollman PA, Case DA, Singh UC, Ghio C, Alagona G, Profeta S, Weiner P. A New Force Field for Molecular Mechanical Simulation of Nucleic Acids and Proteins. *J Am Chem Soc* 1984;106:765.
65. Gasteiger J, Marsili M. Iterative Partial Equalization of Orbital Electronegativity - A Rapid Access to Atomic Charges. *Tetrahedron* 1980;36:3219.
66. Kukla MJ, Breslin HJ, Pauwels R, Fedde CL, Miranda M, Scott MK, Sherrill RG, Raeymaekers A, Van Gelder J, al. e. Synthesis and anti-HIV-1 activity of 4,5,6,7-tetrahydro-5-methylimidazo[4,5,1-jk][1,4]benzodiazepin-2(1H)-one (TIBO) derivatives. *Journal of Medicinal Chemistry* 1991;34(2):746-751.
67. Kukla MJ, Breslin HJ, Diamond CJ, Grous PP, Ho CY, Miranda M, Rodgers JD, Sherrill RG, De Clercq E, al. e. Synthesis and anti-HIV-1 activity of 4,5,6,7-tetrahydro-5-methylimidazo[4,5,1-jk][1,4]benzodiazepin-2(1H)-one (TIBO) derivatives. 2. *Journal of Medicinal Chemistry* 1991;34(11):3187-3197.
68. Breslin HJ, Kukla MJ, Ludovici DW, Mohrbacher R, Ho W, Miranda M, Rodgers JD, Hitchens TK, Leo G, al. e. Synthesis and Anti-HIV-1 Activity of 4,5,6,7-Tetrahydro-5-methylimidazo[4,5,1-jk][1,4]benzodiazepin-2(1H)-one (TIBO) Derivatives. 3. *Journal of Medicinal Chemistry* 1995;38(5):771-793.
69. Ho W, Kukla MJ, Breslin HJ, Ludovici DW, Grous PP, Diamond CJ, Miranda M, Rodgers JD, Ho CY, al. e. Synthesis and Anti-HIV-1 Activity of 4,5,6,7-Tetrahydro-5-methylimidazo[4,5,1-jk][1,4]benzodiazepin-2(1H)-one (TIBO) Derivatives. 4. *Journal of Medicinal Chemistry* 1995;38(5): 794-802.
70. Breslin HJ, Kukla MJ, Kromis T, Cullis H, De Knaep F, Pauwels R, Andries K, De Clercq E, Janssen MAC, Janssen PAJ. Synthesis and anti-HIV activity of 1,3,4,5-tetrahydro-2H-1,4-benzodiazepin-2-one (TBO) derivatives. Truncated 4,5,6,7-tetrahydro-5-methylimidazo[4,5,1-jk][1,4]benzodiazepin-2(1H)-ones (TIBO) analogues. *Bioorganic & Medicinal Chemistry* 1999;7(11): 2427-2436.
71. Solis FJ, EWets RJ-B. Minimization by random search techniques. *Mathematical Operations Research* 1981;6(12):19-30.
72. L'Ecuyer P, Cote S. Implementing a random number package with splitting facilities. *ACM Transactions on Mathematical Software* 1991;17:98-111.
73. Morris GM, Goodsell DS, Halliday RS, Huey R, Hart WE, Belew RK, Olson AJ. Automated Docking Using a Lamarckian Genetic Algorithm and an Empirical Binding Free Energy Function. *J Computational Chemistry* 1998;19:1639-1662.

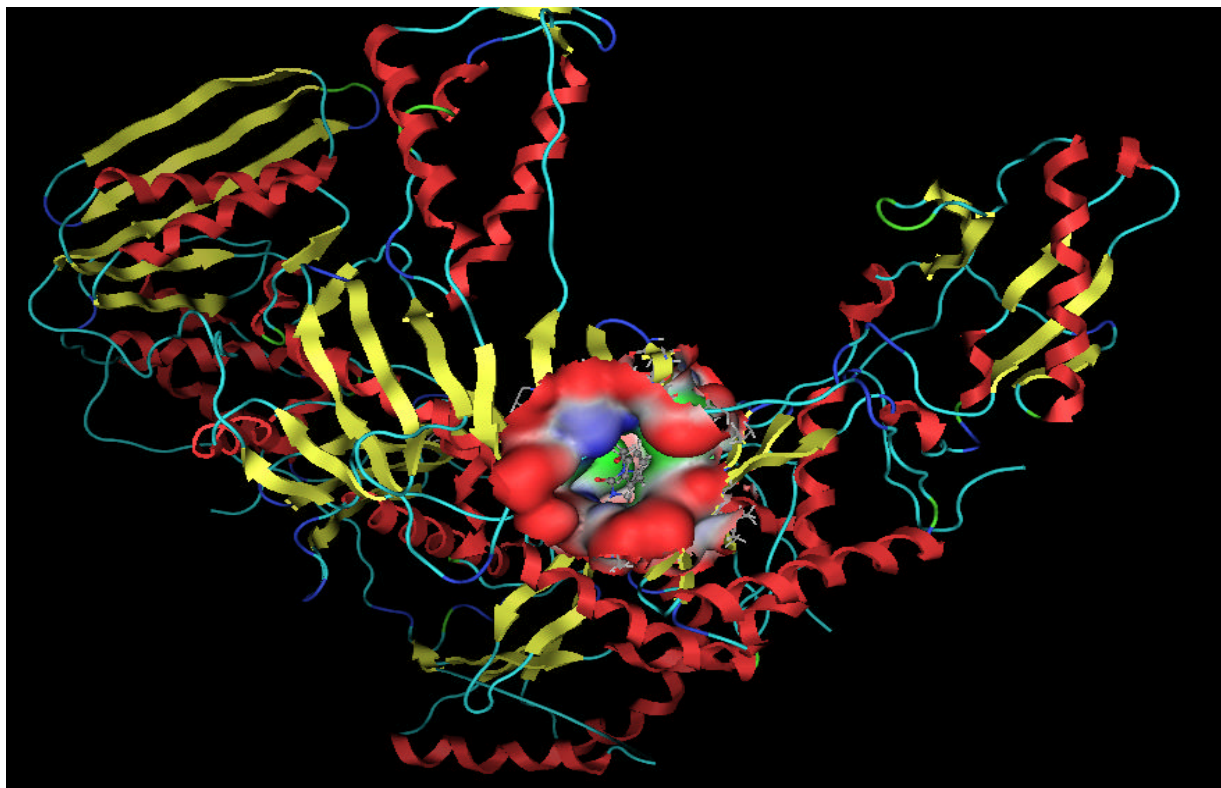


Figure 1. The protein structure of p66 subdomain is colored by secondary structure. 9-Cl-TIBO (colored in green) binds in the NNRTI binding site which is highlighted by a surface enclosed pocket.

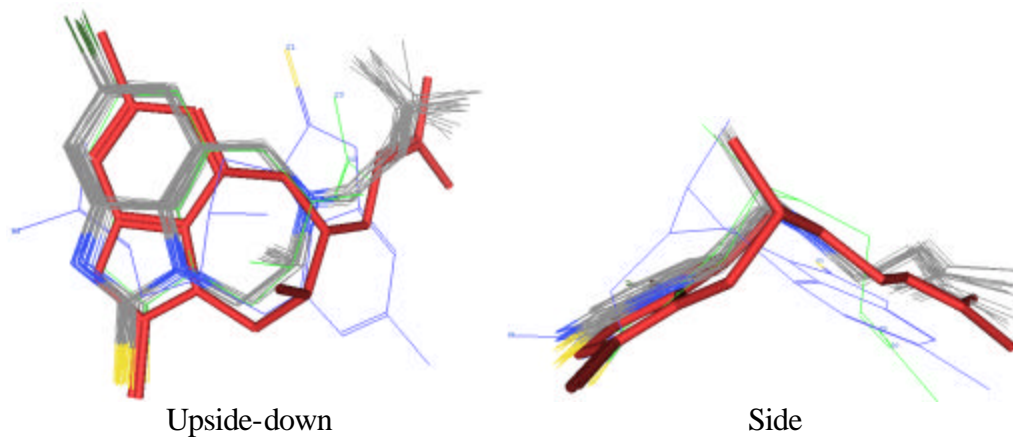


Figure 2. Superposition of all docked configurations (lines) of 9CI-TIBO on crystal structure (red stick). Out of 20, one (blue) has different binding orientation; another (green) has different alkyl chain binding position; all others have very similar binding modes.

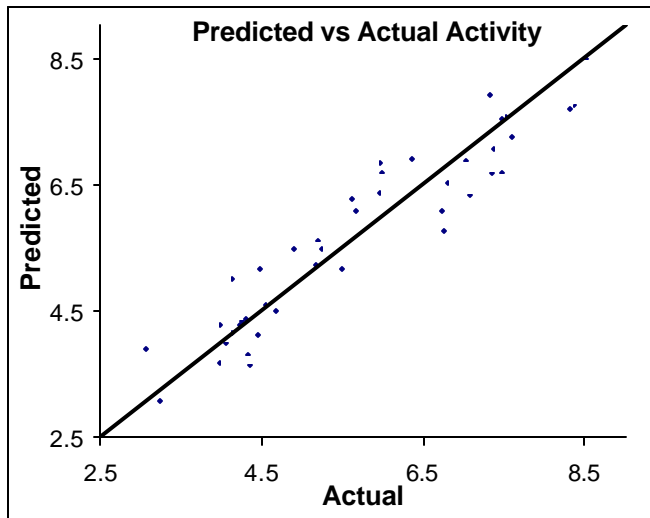


Figure 3. Actual vs. predicted activity values by the free energy equation. The line is perfect model ($Y=X$) and points are data points.

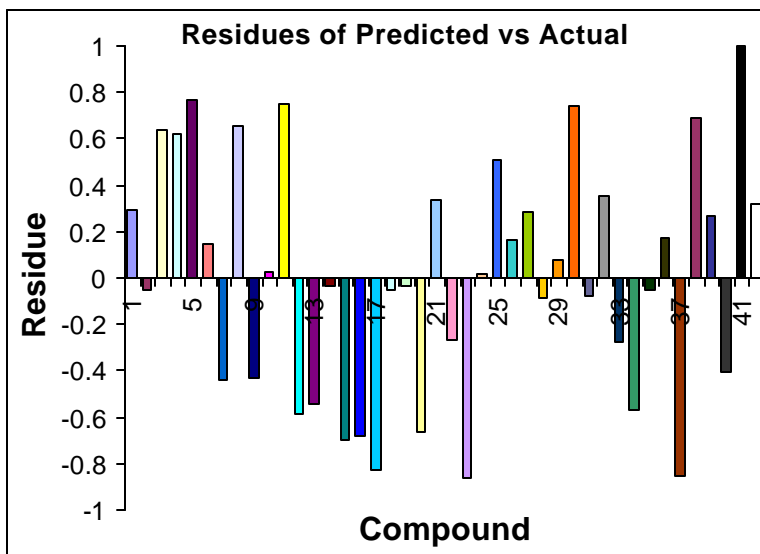


Figure 4. The residues between actual and predicted activities by the final regression model. It can be seen that for nearly all compounds, the difference between the actual activity (pIC_{50}) and the calculated activity is less 1.

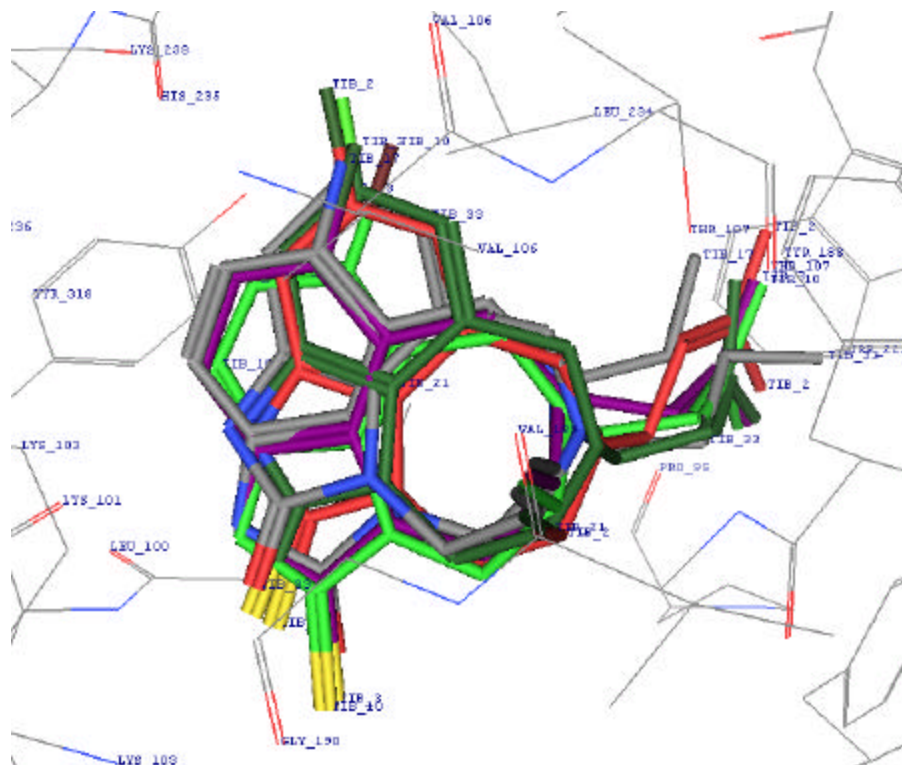
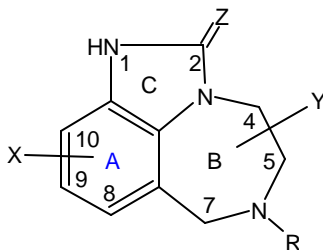


Figure 5. Superposition of six TIBOs from docking results. Four potent ligands with higher pIC_{50} are labeled in different colors: TIBO2 (dark green), TIBO3 (red), TIB10 (light green), and TIBO21 (purple). Two ligands with lower pIC_{50} are colored by element: TIBO26 and TIBO 33.

Table I. Structures and HIV-1 RT Inhibitory Activity of Compounds used in the Work.



compd	X	Z	R	Y	pIC ₅₀
1	H	S	DMA ^a	5-Me(S)	7.36
2	9-Cl	S	DMA	5-Me(S)	7.47
3	8-Cl	S	DMA	5-Me(S)	8.37
4	8-SMe	S	DMA	5-Me(S)	8.30
5	8-OMe	S	DMA	5-Me(S)	7.47
6	8-OC ₂ H ₅	S	DMA	5-Me(S)	7.02
7	8-CN	O	DMA	5-Me(S)	5.94
8	8-CHO	S	DMA	5-Me(S)	6.73
9	8-CONH ₂	O	DMA	5-Me(S)	5.20
10	8-Br	S	DMA	5-Me(S)	8.52
11	8-I	O	DMA	5-Me(S)	7.06
12	8-I	S	DMA	5-Me(S)	7.32
13	8-C=CH	O	DMA	5-Me(S)	6.36
14	8-C=CH	S	DMA	5-Me(S)	7.53
15	8-Me	O	DMA	5-Me(S)	6.00
16	9-NO ₂	O	CPM ^b	5-Me(S)	4.48
17	8-NH ₂	O	CPM ^b	5-Me(S)	3.07
18	9-NH ₂	O	CPM	5-Me(S)	4.22
19	9-NMe ₂	O	CPM	5-Me(S)	5.18
20	9-NO ₂	S	CPM	5-Me(S)	5.61
21	9-F	S	DMA	5-Me(S)	7.60
22	9-CF ₃	O	DMA	5-Me(S)	5.23
23	10-Br	S	DMA	5-Me(S)	5.97
24	H	O	CH ₂ CH=CH ₂	5-Me(S)	4.15
25	H	O	2-MA ^c	5-Me(S)	4.33
26	H	O	CH ₂ CO ₂ Me	5-Me(S)	3.24
27	H	O	CH ₂ -2-furanyl	5-Me(S)	3.97
28	H	O	CH ₂ CH ₂ CH=CH ₂	5-Me(S)	4.30
29	H	O	CH ₂ CH ₂ CH ₃	5-Me(S)	4.05
30	H	O	CPM	5-Me(S)	4.36
31	H	O	CH ₂ CH=CHMe(E)	5-Me(S)	4.24
32	H	O	CH ₂ CH=CHMe(Z)	5-Me(S)	4.46
33	H	O	CH ₂ CH ₂ CH ₂ Me	5-Me(S)	4.00
34	H	O	DMA	5-Me(S)	4.90
35	H	O	CH ₂ C(Me)=CHMe(E)	5-Me(S)	4.54
36	H	O	DMA[R(+)]	5-Me(S)	4.66
37	H	O	CH ₂ C(CH=CH ₂)=CH ₂	5-Me(S)	4.15
38	8-Cl	S	DMA	H	7.34
39	9-Cl	S	DMA	H	6.80
40	9-Cl	S	CPM	4-Me(R)	5.66
41	9-Cl	O	DMA	5-Me(S)	6.74
42	H	O	DMA	5-Me(S)	5.48

^a 3,3-Dimethylallyl. ^b Cyclopropylmethyl. ^c 2-Methylallyl.

Table II. The RMSD and Docking Energies (kcal/mol) from the Docking Simulation of 9Cl-TIBO to its Original Crystal Structure of RT (1REV)

Configuration	RMSD ¹	$\Delta G_{\text{Binding}}$	$\Delta \Delta G_{\text{Binding}}$ ²	ΔE_{Docked}	$\Delta \Delta E_{\text{Docked}}$ ²
1	1.066	-11.04	0	-13.34	0
2	1.032	-11.04	0	-13.34	0
3	0.995	-11.05	-0.01	-13.33	0.01
4	1.036	-11.02	0.02	-13.32	0.02
5	0.988	-11.01	0.03	-13.31	0.03
6	1.057	-11.01	0.03	-13.3	0.04
7	1.022	-10.99	0.05	-13.28	0.06
8	0.908	-11.02	0.02	-13.26	0.08
9	1.052	-11	0.04	-13.26	0.08
10	1.025	-10.94	0.1	-13.25	0.09
11	1.018	-10.96	0.08	-13.23	0.11
12	1.074	-10.96	0.08	-13.23	0.11
13	1.012	-10.91	0.13	-13.22	0.12
14	1.049	-10.96	0.08	-13.22	0.12
15	0.986	-10.95	0.09	-13.22	0.12
16	1.082	-11.01	0.03	-13.21	0.13
17	0.964	-10.87	0.17	-13.12	0.22
18	0.808	-10.91	0.13	-12.84	0.5
19	1.195	-10.61	0.43	-12.99	0.35
20	2.148	-10.6	0.44	-12.21	1.13

1. RMSD, root-mean-square deviation of coordinates between the configuration and initial position (from crystal structure).

2. The energy difference between this configuration and the 1st configuration.

Table III. The Configuration Information in Docking Simulations of All Set of TIBOs to RT.

Compound	# of Cluster ¹	# in major cluster ²	? G _{Binding} ³	Compound	# of Cluster	# in major cluster	? G _{Binding}
1	2	18	-10.8±0.1	22	2	10	-11.7±0.1
2	2	17	-11.0±0.2	23	2	19	-10.7±0.1
3	2	19	-11.4±0.1	24	2	18	-10.1±0.1
4	2	14	-11.3±0.3	25	1	20	-10.2±0.1
5	2	12	-11.1±0.2	26	2	16	-10.2±0.1
6	2	17	-11.9±0.1	27	2	14	-12.2±0.1
7	2	14	-12.6±0.5	28	2	18	-10.5±0.1
8	3	14	-11.6±0.1	29	2	14	-10.0±0.1
9	2	18	-12.1±0.3	30	2	14	-10.1±0.1
10	3	17	-11.2±0.2	31	1	20	-10.5±0.1
11	3	12	-11.5±0.1	32	2	18	-10.6±0.1
12	2	6	-11.3±0.1	33	2	19	-10.5±0.1
13	2	12	-11.3±0.7	34	2	17	-11.0±0.1
14	2	16	-11.9±0.1	35	2	12	-10.5±0.1
15	2	16	-11.4±0.1	36	2	16	-10.6±0.1
16	2	18	-11.2±0.1	37	2	17	-10.8±0.1
17	2	16	-11.2±0.1	38	1	20	-10.7±0.3
18	2	14	-11.3±0.1	39	1	20	-10.3±0.3
19	2	8	-11.3±0.3	40	2	19	-10.8±0.4
20	1	20	-11.0±0.1	41	2	19	-11.1±0.1
21	2	18	-11.1±0.1	42	2	16	-11.4±0.6

1. The number of clusters that all configurations in a docking simulation are grouped.
2. The number of configurations in the major cluster.
3. The free energy of binding from Autodock3, kcal/mol.

Table IV. Calculated Energies and Estimated Binding Free Energy of All Set TIBOs (kcal/mol).

Compound	pIC ₅₀	? G _{vdw}	? G _{ele}	? G _{solv}	SASA	? G _{cald} ¹	pIC _{50,pred} ²
1	7.36	-42.177	-15.143	7.80	-2756.4	-9.63465	7.06352948
2	7.47	-39.123	-12.341	10.25	-2798.1	-10.2646	7.525375
3	8.37	-39.759	-12.693	11.07	-2813	-10.5464	7.731975
4	8.30	-50.872	-9.366	10.24	-2803.1	-10.4771	7.681158
5	7.47	-47.197	-16.021	11.39	-2800.5	-9.14108	6.701672
6	7.02	-49.258	-18.76	11.79	-2824.4	-9.37238	6.871243
7	5.94	-41.456	-17.388	12.75	-2789.9	-8.70028	6.378501
8	6.73	-44.483	-20.383	16.18	-2796.7	-8.29043	6.07803
9	5.20	-48.047	-19.574	12.80	-2780.7	-7.67799	5.629025
10	8.52	-39.285	-12.279	11.43	-2833.6	-11.5912	8.4979658
11	7.06	-44.541	-14.968	8.46	-2778.9	-8.60382	6.307787
12	7.32	-43.827	-11.371	7.27	-2818.1	-10.7816	7.904388
13	6.36	-42.376	-14.112	12.73	-2791.5	-9.41292	6.900971
14	7.53	-44.011	-14.229	12.71	-2818.7	-10.3196	7.565683
15	6.00	-42.903	-10.061	11.53	-2761.9	-9.14114	6.701719
16	4.48	-43.136	-21.866	5.32	-2776.1	-7.03394	5.156844
17	3.07	-46.687	-18.279	8.52	-2709.7	-5.32	3.900292
18	4.22	-40.793	-19.326	7.32	-2724.9	-5.83215	4.275771
19	5.18	-45.185	-23.258	16.55	-2781.2	-7.10771	5.210929
20	5.61	-42.635	-17.695	8.62	-2791.4	-8.55653	6.273113
21	7.60	-35.885	-19.656	7.04	-2834.4	-9.90902	7.264679
22	5.23	-35.995	-25.632	7.76	-2802.1	-7.49371	5.493921
23	5.97	-40.673	-16.023	11.93	-2798.8	-9.3191	6.832183
24	4.15	-41.399	-12.22	7.28	-2679.1	-5.63545	4.131563
25	4.33	-39.094	-18.976	9.45	-2702.8	-5.20934	3.819162
26	3.24	-39.975	-16.22	8.85	-2660.1	-4.1908	3.072431
27	3.97	-52.19	-18.586	6.93	-2709.6	-5.02388	3.683194
28	4.30	-42.497	-17.585	7.24	-2720.8	-5.98688	4.389205
29	4.05	-39.208	-14.65	6.80	-2685.2	-5.41339	3.968761
30	4.36	-40.423	-17.943	8.09	-2691.4	-4.93458	3.617725
31	4.24	-44.273	-12.58	5.40	-2692	-5.88624	4.315422
32	4.46	-41.327	-14.879	7.79	-2693.1	-5.60067	4.106066
33	4.00	-42.537	-13.204	8.02	-2690.8	-5.83122	4.275089
34	4.90	-42.803	-13.86	9.10	-2739	-7.46082	5.469811
35	4.54	-40.716	-16.253	8.21	-2718.4	-6.26304	4.591669
36	4.66	-42.192	-14.943	7.44	-2708.8	-6.11991	4.486736
37	4.15	-45.65	-12.563	7.68	-2717.7	-6.8271	5.005208
38	7.34	-40.063	-13.291	6.81	-2778.9	-9.07511	6.653307
39	6.80	-42.969	-15.785	8.79	-2790.4	-8.91291	6.534389
40	5.66	-38.743	-14.753	8.33	-2762.9	-8.26707	6.060904
41	6.74	-41.082	-16.933	8.46	-2765.7	-7.83276	5.742496
42	5.48	-45.285	-13.279	6.99	-2727.6	-7.03412	5.156976

1. Calculated free energy of binding, ? G_{cald} is calculated from optimized linear combination of ? G_{ele}, ? G_{vdw}, ? G_{solv}, and SASA from regression.
2. Predicted pIC₅₀ is estimated from ? G_{cald} using the following relationship: ? G_{binding} = RTlnK_{dissociated} ~ RTlnIC₅₀ = -RTpIC₅₀, where 298K is used in the work for temperature T.

Table V. Regression Properties of Final Free Energy of Binding vs Activity of TIBOs.

	pIC ₅₀	? G _{vdw}	? G _{ele}	? G _{solv}	SASA
Correlation Factor with pIC ₅₀	1.00	.22	-.08	.38	.86
	Intercept				
B	-64.45	.0256	0.1538	0.0164	-0.0267
St. Err. of B	5.725	0.02670	0.02673	0.04010	0.002092
Correlation coefficient, $r = 0.9317$; $r^2 = 0.8680$			$F = 55.902$; $p < 0.00000$		
Cross-validation coefficient,			$q = 0.9109$; $q^2 = 0.8298$		